Spatio-Temporal Trajectory-Driven Dynamic TDMA Scheduling for UAV-Assisted Wireless-Powered Communication Networks

Siliang Gong , Kaiyang Qu , Hongfei Wang , Yaopei Wang , Hanyao Huang , Peixin Qu , Qinghua Chen *

Posted Date: 28 March 2026

doi: 10.20944/preprints202603.2180.v1

Keywords: wireless powered communication network; unmanned aerial vehicle; spatial-temporal trajectory prediction; time-division multiple access scheduling

Article

Spatio-Temporal Trajectory-Driven Dynamic TDMA Scheduling for UAV-Assisted Wireless-Powered Communication Networks

Siliang Gong [1], Kaiyang Qu [1], Hongfei Wang [1], Yaopei Wang [1], Hanyao Huang [1], Peixin Qu [2] and Qinghua Chen [3,*]

[1] School of Computer and Software, Nanyang Institute of Technology, Nanyang, Henan 473306, China
[2] School of Information Engineering, Henan Institute of Science and Technology, Xinxiang, Henan 453003, China
[3] School of Artificial Intelligence, Wenzhou Polytechnic, Wenzhou, Zhejiang, 325000, China
* Correspondence: kegully@qq.com

Abstract

UAV-assisted data collection often suffers from spatial data holes and communication unfairness, a challenge exacerbated in Wireless Powered Communication Networks (WPCNs) by the inherent doubly near-far problem. To bridge these gaps, this paper proposes a novel Spatio-Temporal Trajectory-Driven Dynamic Time-Division Multiple Access (STD-TDMA) scheduling strategy. Deviating from conventional discrete hovering paradigms, we introduce a continuous-flight framework that exploits the UAV's mobility to provide seamless spatial coverage. By jointly optimizing the UAV's flight speed and dynamic time-slot allocation, the proposed strategy ensures that each sensor node can interact with the UAV at its optimal channel condition along the trajectory, thereby effectively mitigating the doubly near-far effect and ensuring absolute nodal fairness. To solve the formulated non-convex optimization problem, we develop a low-complexity algorithm that integrates Binary Search for speed optimization with the Hungarian algorithm for spatio-temporal mapping. Extensive simulations demonstrate that our STD-TDMA strategy significantly enhances nodal fairness and boosts overall task execution efficiency compared to conventional baseline schemes.

Keywords: wireless powered communication network; unmanned aerial vehicle; spatial-temporal trajectory prediction; time-division multiple access scheduling

1. Introduction

In recent years, Unmanned Aerial Vehicles (UAVs) have been extensively deployed for data collection in Internet of Things (IoT) and Wireless Sensor Networks (WSNs). Owing to their high flexibility, rapid deployment capabilities, and controllable mobility, UAVs can establish line-of-sight (LoS) communication links with ground sensor nodes, significantly enhancing network coverage and connectivity[1,2].

However, traditional UAV-assisted data collection often relies on a "hovering-and-gathering" paradigm, where the UAV flies to predetermined locations and hovers to interact with ground nodes [3]. This static communication mode inevitably leads to a severe spatial discrepancy: nodes located near the hovering point enjoy excellent channel conditions and collect massive amounts of data, while edge nodes suffer from severe path loss. This issue is critically exacerbated in UAV-assisted Wireless Powered Communication Networks (WPCNs). In such energy-harvesting scenarios, edge nodes not only harvest significantly less radio frequency (RF) energy but also require more power to transmit data over longer distances. This cascading effect, known as the "doubly near-far problem"[4], results in severe unfairness and creates spatial "data holes," where the basic data demands of distant nodes are entirely neglected.

 doi:10.20944/preprints202603.2180.v1

Furthermore, the traditional hovering paradigm heavily degrades task execution efficiency, as the flight time between hovering waypoints is strictly wasted without any communication payload. To overcome this inefficiency, enabling the UAV to communicate while flying is a promising approach. Nevertheless, the continuous movement of the UAV introduces highly dynamic spatio-temporal variations in channel states along the flight trajectory. To fully exploit the UAV's mobility without compromising fairness, it is imperative to design an efficient multi-access scheduling strategy. A rigid or fixed communication sequence cannot adapt to these spatial-temporal changes, making dynamic resource scheduling based on the continuous trajectory essential for guaranteeing fairness and maximizing task efficiency.

Motivated by the aforementioned challenges, this paper proposes a novel multi-access scheduling strategy, termed Spatio-Temporal Trajectory-Driven Dynamic Time-Division Multiple Access (STD-TDMA), for UAV-assisted WPCNs. Deviating from the conventional discrete hovering paradigm, the UAV employs a continuous "fly-and-communicate" mechanism. By synergizing spatio-temporal trajectory prediction with dynamic resource allocation, STD-TDMA aims to mitigate the inherent doubly near-far problem, thereby reconciling the fundamental trade-off between communication fairness and data collection efficiency. The main contributions of this paper are summarized as follows:

- We propose the STD-TDMA continuous-flight framework to strictly guarantee the communication quality of all nodes, thereby effectively eliminating spatial data holes. By replacing rigid hovering points with a continuous trajectory, the proposed framework exploits the spatio-temporal diversity of the UAV's mobility. This structurally addresses the doubly near-far problem by allowing each sensor node to be scheduled at its most advantageous spatial position, ensuring that no node is disadvantaged by its geographic location.
- To evaluate the trade-off between task execution efficiency and communication performance, we formulate a joint optimization problem. The problem aims to maximize the average system throughput rate by jointly optimizing the UAV's continuous flight speed and the dynamic TDMA scheduling, subject to strict Quality of Service (QoS) constraints for all nodes to ensure absolute fairness.
- We propose a low-complexity, two-tier decoupled algorithm to tackle the highly non-convex and combinatorial nature of the formulated problem. Specifically, the outer layer utilizes a bisection search to determine the critical optimal continuous flight speed by exploiting the proven monotonic property, while the inner layer dynamically transforms the multi-access scheduling into a maximum weight matching problem, which is optimally solved via the Hungarian algorithm leveraging spatio-temporal trajectory states.
- Simulations are conducted to validate the proposed STD-TDMA. Compared with conventional baseline schemes, our STD-TDMA demonstrates significant superiority in guaranteeing nodal fairness, eliminating data holes, and boosting overall data collection efficiency.

The rest of this paper is organized as follows. Section 2 reviews the related work. Section 3 describes the system model, and Section 4 formulates the optimization problem. The proposed solution is detailed in Section 5. Simulation results and discussions are provided in Section 6. Finally, Section 7 concludes the paper and discusses future work.

2. Related Work

2.1. UAV Trajectory Optimization and Data Collection

In recent years, UAVs have emerged as versatile mobile data collectors in WSNs due to their high mobility and flexibility. Gu and Zhang [5] provided a comprehensive overview of diverse UAV applications, categorizing their roles as mobile terminals, aerial base stations, and relays. Zeng *et al.* [6] systematically investigated the throughput maximization problem for a UAV-enabled mobile relaying system, demonstrating that a dynamic "fly-and-communicate" trajectory significantly outperforms conventional static relaying. Building upon this, Wu *et al.* [7] explored a multi-UAV enabled wireless network, where trajectory and communication were jointly optimized to maximize the minimum

 doi:10.20944/preprints202603.2180.v1

throughput. Subsequently, extensive efforts have been made to optimize UAV trajectories for efficient data collection in Internet of Things (IoT) networks [8]. For instance, deep reinforcement learning approaches have been actively deployed to autonomously design UAV trajectories in complex environments [9]. Furthermore, recent studies have begun incorporating ambient energy harvesting into UAV systems to reduce carbon footprints and improve propulsion energy efficiency [10,11]. While these works established the foundation of UAV mobility, they primarily focused on active transmission scenarios without fully addressing the stringent energy constraints inherent in self-sustaining sensor networks.

2.2. UAV-Enabled WPCNs and Energy Harvesting

To prolong the operational lifespan of low-power IoT devices, Wireless Powered Communication Networks (WPCNs) have been widely investigated [12]. By deploying UAVs as mobile energy transmitters and data collectors, the spatial limitations of fixed access points can be effectively mitigated. Nevertheless, UAV-WPCNs inherently suffer from the severe "doubly near-far problem," where distant nodes harvest less energy but require more power to transmit data. To tackle this, Xie *et al.* [13] investigated throughput maximization in UAV-enabled WPCNs and proposed a "successive hover-and-fly" trajectory. To further mitigate this distance-dependent signal attenuation, Cho *et al.* [14] proposed a weighted harvest-then-transmit protocol. Additionally, Li *et al.* [15] and Luo *et al.* [16] explored joint three-dimensional (3D) trajectory and power/time allocation optimizations to enhance the energy utilization efficiency of UAVs under obstacle constraints. Similar data-gathering scenarios over fading channels and 3D environments have also been extensively evaluated [17–19]. Wu *et al.* [20] studied covert communications in a UAV-enabled network, focusing on maximizing the minimum throughput among ground users by jointly optimizing the UAV's trajectory, transmit power, and power allocation coefficient, under UAV mobility and covertness constraints. Although these studies optimize WPT efficiency and mitigate the near-far effect to some extent, many of them still rely on the time-consuming "hovering" mechanism [13,19], which inevitably wastes substantial flight time and degrades the overall data collection efficiency.

2.3. Dynamic Multi-Access Scheduling and Fairness

To fully exploit continuous UAV flight without compromising nodal fairness, dynamic multi-access scheduling becomes indispensable. Rigid scheduling fails to adapt to the highly dynamic spatial-temporal channel variations caused by the UAV's movement. Lyu *et al.* [21] explored resource allocation in UAV-enabled orthogonal frequency division multiple access (OFDMA) systems, introducing a minimum-rate ratio to guarantee delay constraints and revealing a fundamental throughput-delay tradeoff. In WPCNs, ensuring that every node receives a fair share of data collection is critical. An *et al.* [22] proposed joint scheduling and trajectory optimization to minimize total execution time. Meanwhile, Park *et al.* [23] and Tang *et al.* [24] focused on maximizing the minimum throughput (Max-Min fairness) among all users to guarantee that edge nodes are not entirely neglected. Recently, scheduling fairness and communication security have also been jointly investigated in multi-UAV mobile edge computing systems [25,26]. However, integrating dynamic multi-access scheduling with continuous, non-hovering flight trajectories mathematically leads to highly non-convex combinatorial optimization problems, which are notoriously difficult to solve with low computational complexity.

Different from the aforementioned literature that either relies on time-consuming hovering paradigms [13,20] or employs computationally prohibitive centralized algorithms, this paper introduces a novel continuous-flight WPCN framework. By actively predicting spatial-temporal trajectory states, we propose a low-complexity two-stage decoupled algorithm to dynamically optimize the flight speed and TDMA scheduling, structurally eliminating spatial data holes and guaranteeing absolute fairness while maximizing data collection efficiency.

 doi:10.20944/preprints202603.2180.v1

3. System Model

3.1. Network Model

As illustrated in Figure 1, we consider a UAV-assisted wireless powered communication network, where the service area is partitioned into M regular hexagonal cells, denoted by $\mathcal{M} = \{1, 2, \ldots, M\}$. Considering a 3D Cartesian coordinate system, the 3D center coordinate of cell $m \in \mathcal{M}$ is represented as $\mathbf{c}_m = (x_m, y_m, 0)$. Each cell m contains a set of S_m sensor nodes (SNs), denoted by $\mathcal{K}_m = \{1, 2, \ldots, S_m\}$. These SNs are randomly deployed within the cell. Let $S_{k,m}$ denote the k-th ($k \in \mathcal{K}_m$) sensor node in cell m, and $s_{k,m} = (x_{k,m}, y_{k,m}, 0) \in \mathbb{R}^3$ denote the location of $S_{k,m}$. The UAV functions as a mobile Hybrid Access Point (HAP) in this work, providing energy to sensor nodes via downlink charging and performing uplink data collection. The UAV traverses a sequence of hexagonal cells maintains a constant velocity, denoted as v_m. Its instantaneous 3D position is denoted as $\mathbf{q}(t) = (x(t), y(t), H)$, where H represents the constant flight altitude. For each hexagonal cell $m \in \mathcal{M}$, the SN follows a localized "harvest-then-transmit" protocol. Sensor nodes equipped with energy harvesting (EH) modules first collect energy from the RF signals transmitted by the UAV. Subsequently, they sense the ambient environment, generate data, and transmit the produced data to the UAV by consuming the harvested energy. Without loss of generality, we assume that the UAV has sufficient energy to complete one round of data collection.

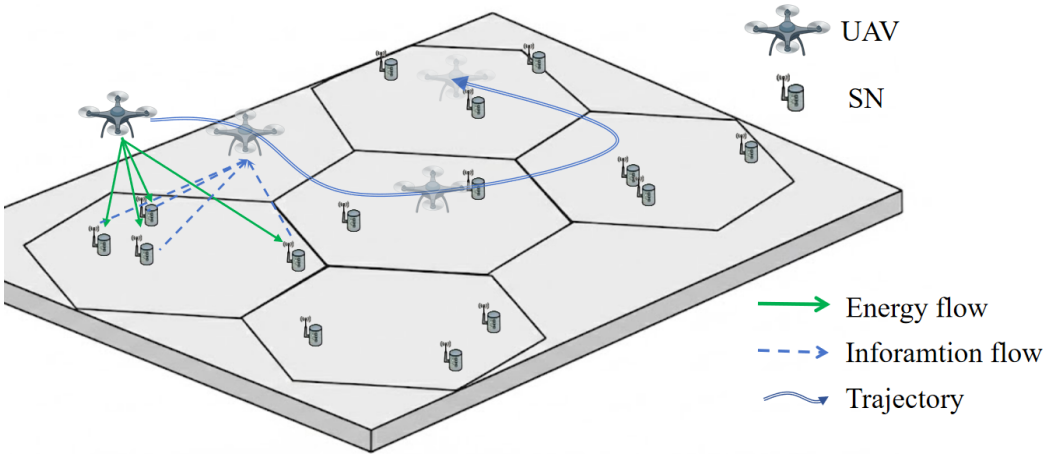

Figure 1. The UAV-assisted WPCN.

In this paper, we assume that the trajectory of the UAV is predetermined, therefore, path planning is not addressed in this work. Upon entering each cell $m \in \mathcal{M}$, the UAV executes a localized two-phase protocol: it first performs downlink wireless energy transfer (WET) to broadcast energy to all sensor nodes within the cell. Subsequently, it transitions to the wireless information transmission (WIT) phase, where it gathers uplink information from each sensor node in the current cell via a time-division multiple access (TDMA) scheme. During the WIT phase, each node occupies one TDMA time slot for data transmission. Let T_m denote the total dwell time of the UAV in cell m. The dwell period T_m is divided into $2N_m$ time slots with equal duration $\tau_m = T_m/2N_m$, which is considered to be sufficiently small to ensure that the positions of UAV to be unchanged and the channel state remains constant within each time slot. In addition, we have

$$T_m = \frac{D}{v_m}, \tag{1}$$

where D denote the distance traversed by the UAV within each cell. It is given by

$$D = \sqrt{3}R, \tag{2}$$

 doi:10.20944/preprints202603.2180.v1

where R is the side length of each regular hexagonal cell.

3.2. Channel Model

In the considered WPCN, the communication links between the UAV and the ground nodes during its flight may be obstructed by obstacles such as trees or terrain, leading to the possible presence of both line-of-sight and non-line-of-sight (NLoS) links. To accurately characterize the propagation environment, the air-to-ground (A2G) channel model from [27,28] is employed, which accounts for the probabilistic occurrence of LoS and NLoS links.

Given the coordinates described above, the Euclidean distance $d_{k,m}(t)$ between the UAV and the k-th SN located in the m-th cell at time instant t is expressed as

$$d_{k,m}(t) = \sqrt{||\mathbf{q}(t) - s_{k,m}||^2}. \tag{3}$$

The LoS probability is determined by the elevation angle (in degrees), which is defined as the angle formed between the horizontal plane and the line connecting the UAV to the ground SN. At time instant t, the elevation angle $\theta_{m,k}(t)$ with respect to the k-th sensor in cell m can be expressed as

$$\theta_{m,k}(t) = \frac{180}{\pi} \arcsin\left(\frac{H}{d_{m,k}(t)}\right). \tag{4}$$

As in [27], the probability of the existence of a LoS link, denoted as $P_{LoS,m,k}(t)$, is given by

$$P_{LoS,m,k}(t) = \frac{1}{1 + a\exp(-b[\theta_{m,k}(t) - a])}, \tag{5}$$

where a and b are environment-dependent constants [29] (e.g., urban, suburban). Thus, the average power gain $h_{m,k}(t)$ between the UAV and the k-th node in cell m is given by

$$h_{m,k}(t) = P_{LoS,m,k}(t)h_{LoS,m,k}(t) + [1 - P_{LoS,m,k}(t)]\eta h_{LoS,m,k}(t), \tag{6}$$

where $\eta \in (0, 1]$ represents the additional attenuation factor of the NLoS link. $h_{\mathrm{LoS},m,k}(t)$ represents the channel power gain of the LoS link, which follows the free-space path loss model, given by $h_{\mathrm{LoS},m,k}(t) = \beta_0 d_{m,k}^{-\delta}(t)$. Here, β_0 denotes the channel power gain at the reference distance of 1 m, and δ represents the path loss exponent.

3.3. Energy Model

As illustrated in Figure 2, under the STD-TDMA, upon entering any cell $m \in \mathcal{M}$, the UAV first allocates N_m consecutive time slots for downlink WET, followed by the remaining N_m slots for uplink data collection. The duration of each time slot is assumed to be sufficiently small such that the UAV's position remains quasi-static within each individual slot.

 doi:10.20944/preprints202603.2180.v1

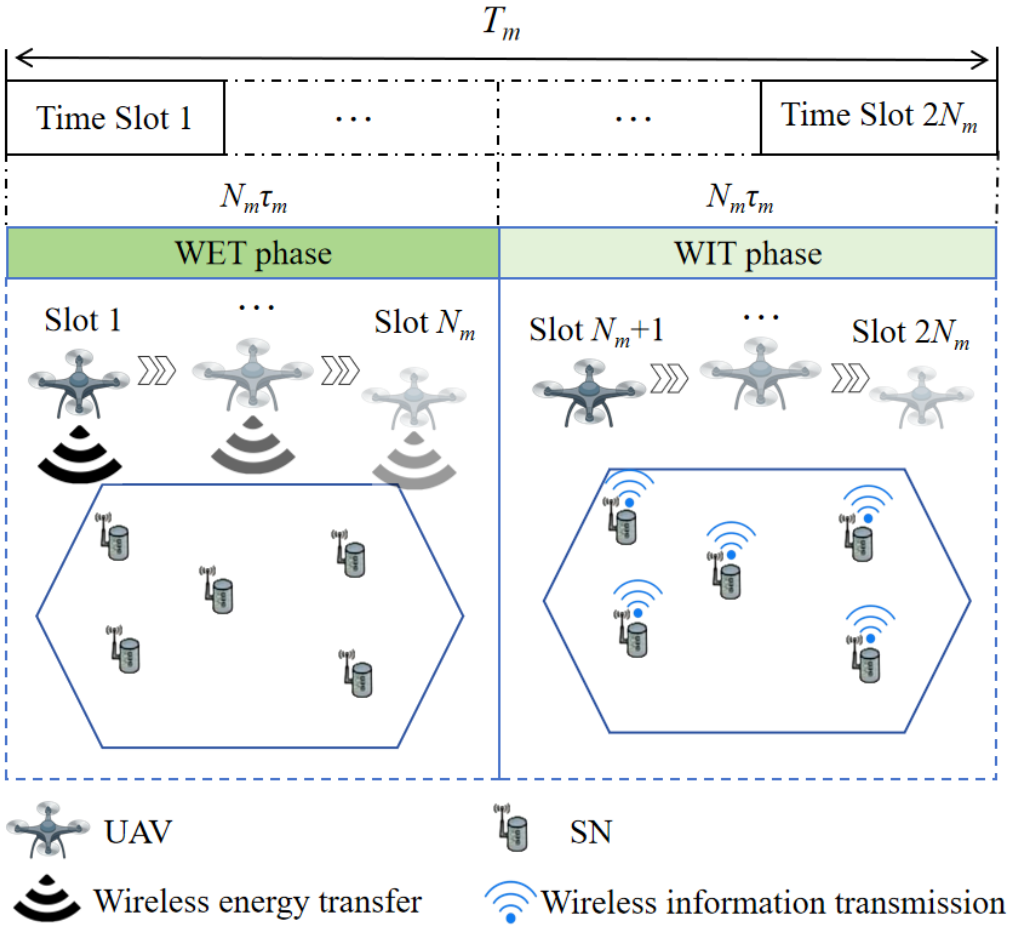

Figure 2. TDMA based on UAV-assisted WPCN.

During the WET phase, the UAV broadcasts RF signals with a constant power P_e to all nodes in the cell. It is important to note that the UAV's position varies continuously over time, leading to time-dependent channel gains between the UAV and the SNs. Consequently, after N_m time slots, the total energy harvested by node $k \in \mathcal{K}_m$ is formulated as

$$E_{m,k} = \zeta \sum_{t=0}^{N_m\tau_m} P_e h_{m,k}(t)\tau_m. \tag{7}$$

Here, $\zeta \in (0,1]$ denotes the energy conversion efficiency, whose value is contingent upon the specific hardware design of the energy harvesting circuitry.

During the WIT phase, sensor nodes utilize the harvested energy to transmit their collected data to the UAV through the uplink. The time and energy consumption for environmental sensing are assumed to be negligible. For throughput maximization in energy-limited systems, it is optimal for a node to deplete its total harvested energy at a constant power level throughout the assigned transmission interval [30]. Thus, we have

$$p_{m,k} \leq \frac{E_{m,k}}{\tau_m}, \tag{8}$$

where $p_{m,k}$ is the transmit power of node k in cell m.

It should be noted that the UAV's position varies continuously over time. Consequently, the instantaneous throughput (achievable rate) of node $k \in \mathcal{K}_m$ at time t is given by

$$R_{m,k}(t) = B\log_2\left(1 + \frac{p_{m,k}h_{m,k}(t)}{\sigma^2}\right). \tag{9}$$

 doi:10.20944/preprints202603.2180.v1

Here, B represents the network bandwidth and σ^2 is the additive white Gaussian noise power at the UAV receiver.

4. Problem Formulation

The proposed STD-TDMA aims to improve the UAV's mission execution efficiency while simultaneously ensuring the communication QoS for the sensor nodes. Specifically, this is achieved by jointly optimizing the UAV's flight velocities $\mathbf{v} = \{v_m\}$ across various cells and the corresponding intra-cell TDMA assignment matrix $\mathbf{X} = \{\mathbf{X}_m\}$, thereby navigating the inherent trade-off between throughput gains and temporal costs.

Following the TDMA protocol, each node is allocated a single time slot during the WIT phase for data transmission. Assuming that the i-th TDMA time slot is allocated to node k, the amount of data (in bits) collected by the UAV from this node is given by

$$\Phi_{m,k}(i) = \int_{(N_m+i-1)\tau_m}^{(N_m+i)\tau_m} R_{m,k}(t)dt, i \in \{1, \ldots, N_m\}. \tag{10}$$

Let $x_{i,k}^m$ be an indicator for whether slot i is assigned to node k in cell m. Consequently, the TDMA assignment matrix is a binary matrix, denoted by $\mathbf{X}_m = [x_{i,k}^m]_{N_m \times S_m}$, where each element is defined as

$$x_{i,k}^m = \begin{cases} 1, & \text{if slot } i \text{ is assigned to node } k, \\ 0, & \text{otherwise.} \end{cases} \tag{11}$$

Thus, the cumulative throughput of node k in cell m is denoted by

$$\Phi_{m,k} = \sum_{i=1}^{N_m} x_{i,k}^m \Phi_{m,k}(i). \tag{12}$$

To evaluate the trade-off between communication performance and mission execution efficiency, we define the system utility function as the average system throughput rate. This is formulated as the ratio of the total collected data to the total mission execution time, expressed as

$$\mathcal{U} = \frac{\sum_{m=1}^{M} \sum_{k=1}^{S_m} \Phi_{m,k}}{\sum_{m=1}^{M} \frac{D}{v_m}}. \tag{13}$$

Here, the numerator quantifies the overall communication performance in terms of the total data collected from all nodes, while the denominator characterizes the total mission execution time of the UAV. Optimizing this fractional metric intrinsically maximizes the data collection efficiency.

 doi:10.20944/preprints202603.2180.v1

Based on the defined system utility, our objective is to maximize the data collection efficiency by jointly optimizing the UAV cruising velocity set $\mathbf{v} = \{v_m\}_{m=1}^{M}$ and the time-slot scheduling matrix $\mathbf{X} = \{\mathbf{X}_m\}_{m=1}^{M}$. Accordingly, the optimization problem is formulated as follows.

$$
\begin{aligned}
(\mathrm{P1}) \quad \max_{\mathbf{v},\mathbf{X}} \quad & \mathcal{U} \\
\text{s.t.} \quad & \Phi_{m,k} \geq R_{th}, \quad \forall m \in \mathcal{M}, k \in \mathcal{K}_m, && \text{(14a)} \\
& v_{\min} \leq v_m \leq v_{\max}, \quad \forall m \in \mathcal{M}, && \text{(14b)} \\
& \tau_m = \frac{D}{2N_m v_m}, && \text{(14c)} \\
& p_{m,k}\tau_m \leq E_{m,k}, \quad \forall m \in \mathcal{M}, k \in \mathcal{K}_m, && \text{(14d)} \\
& p_{m,k} \leq P_{max}, \quad \forall m \in \mathcal{M}, k \in \mathcal{K}_m, && \text{(14e)} \\
& \sum_{i=1}^{N_m} x_{i,k} \leq 1, \quad \forall k \in \mathcal{K}_m, && \text{(14f)} \\
& \sum_{k \in \mathcal{K}_m} x_{i,k} \leq 1, \quad \forall i \in \{1, \ldots, N_m\}. && \text{(14g)}
\end{aligned}
$$

Here, constraint (14a) represents the QoS requirement, ensuring that the cumulative throughput of each node is no less than the threshold R_{th}. Constraint (14b) restricts the UAV flight velocity within a practical operational range. $v_{\min}$ and $v_{\max}$ denote the minimum and maximum flight speeds of the UAV, respectively. Constraint (14d) and (14e) denote the energy and power constraints of the nodes, respectively. Constraint (14f) and (14g) enforce the uniqueness of the TDMA scheduling, ensuring that each node is allocated at most one WIT slot and each slot serves at most one node.

5. Problem Solution

Problem (P1) is a Mixed-Integer Non-Linear Programming (MINLP) problem due to the fractional objective function, the continuous velocity variables, and the binary scheduling indicators. Finding the global optimum through conventional methods is computationally prohibitive. Before introducing the solution approach, we first present two theorems.

Theorem 1. *In the absence of QoS constraints, the average system utility $\mathcal{U}$ remains constant regardless of the UAV cruising velocity v_m.*

Proof of Theorem 1. Without loss of generality, we consider a single cell m with a fixed trajectory distance D. When the UAV cruises at a constant velocity V_m, the total mission time is $T_m = D/V_m$. By discretizing the trajectory into a set of time slots, the duration of a single slot is given by $\tau_m \propto T \propto 1/V_m$.

As indicated in (7), the harvested energy of node k is defined as the integral of the node's received RF power over the duration of the EH slots. Since the spatial trajectory of the UAV is predetermined, the instantaneous received power $P_e h_{m,k}(t)$ is exclusively determined by the geometric location and represents a spatial constant independent of the velocity V. Let $\alpha_{m.k} = \sum_t \zeta P_e h_{m,k}(t)$, then $E_{m,k} = \alpha_{m.k}\tau_m$.

In the WIT phase, the actual transmit power $p_{m,k}$ of node k is constrained by both its harvested energy and the hardware limitation $P_{\max}$:

$$
p_{m,k} = \min\left(\frac{E_{m,k}}{\tau_m}, P_{\max}\right) = \min\left(\frac{\alpha_{m.k}\tau_m}{\tau_m}, P_{\max}\right) = \min(\alpha_{m.k}, P_{\max}). \tag{15}
$$

Observe that the time component τ_m is perfectly canceled out. Thus, $p_{m,k}$ is a constant independent of V_m. Consequently, according to the Shannon capacity formula, the instantaneous transmission rate $R_{m.k} = B\log_2(1 + p_{m,k}H_{m,k}/\sigma^2)$ is also a constant.

 doi:10.20944/preprints202603.2180.v1

Finally, the system average utility $\mathcal{U}_m$ is given by the ratio of the total throughput to the total time:

$$\mathcal{U}_m = \frac{\sum_{k=1}^{S_m} R_{m,k}\tau_m}{T_m}. \tag{16}$$

Since both the numerator (total throughput) and the denominator (total time T) scale proportionally with $1/V_m$, the average utility $\mathcal{U}$ remains strictly constant. This completes the proof. □

Theorem 2. *Under the given time-slot allocation policy, the throughput $\Phi_{m,k}$ of each sensor node k in cell m is a strictly monotonically decreasing function of the UAV cruising velocity v_m.*

Proof. As established in Theorem 1, the transmit power $p_{m,k}$ and the corresponding instantaneous transmission rate $R_{m,k}$ are independent of the velocity v_m due to the perfect cancellation of the time component τ_m. Specifically, the throughput $\Phi_{m,k}$ defined in (12) can be re-expressed as a function of the UAV cruising velocity v_m as follows

$$\Phi_{m,k}(v_m) = R_{m,k} \cdot \tau_m = R_{m,k} \cdot \frac{D}{2N_m v_m}. \tag{17}$$

By taking the first-order derivative of $\Phi_{m,k}$ with respect to v_m, we obtain:

$$\frac{d\Phi_{m,k}(v_m)}{dv_m} = -\frac{R_{m,k}D}{2N_m v_m^2}. \tag{18}$$

Given that the transmission rate $R_{m,k}$, the trajectory distance D, and the number of slots N are all positive physical constants, it follows that $\frac{d\Phi_{m,k}(v_m)}{dv_m} < 0$ for all $v_m > 0$. This proves that the individual throughput $\Phi_{m,k}$ decreases strictly as the velocity v_m increases. □

Theorem 1 reveals that optimizing velocity for average utility is mathematically trivial, shifting the design focus to identifying the maximum feasible velocity v_m^* that tightly satisfies the QoS constraint. Meanwhile, Theorem 2 establishes the strict monotonicity of individual throughput with respect to v_m, ensuring that the feasible velocity region is contiguous and well-defined. Building upon these theoretical insights, we propose a decoupled two-tier optimization framework. Specifically, the inner layer determines the optimal assignment matrix $\mathbf{X}^*$ to maximize throughput for a given velocity, while the outer layer utilizes a bisection search to converge to the critical velocity v_m^*. This iterative process is theoretically guaranteed to converge due to the monotonic relationship proven in Theorem 2.

5.1. Inner Layer: Task Assignment

For a given flight velocity v_m, the optimization problem (P1) reduces to a linear assignment task. To quantify the potential data harvested from each sensor, we construct a cost matrix $\mathbf{C}_m \in \mathbb{R}^{N_m \times S_m}$. Each element $C_{i,k}^m$ represents the predicted throughput of node k during WIT slot $i \in \{1, \ldots, N_m\}$, which is pre-calculated using the predicted UAV coordinates $\mathbf{q}(i)$ and the resulting time-varying channel gain $h_{i,k}$.

To strictly enforce the QoS requirement, we perform a pruning operation on the cost matrix. Any assignment that fails to meet the minimum threshold R_{th} is penalized with a weight of negative infinity, ensuring the algorithm prioritizes feasible solutions

$$\tilde{C}_{i,k}^m = \begin{cases} C_{i,k}^m, & \text{if } C_{i,k} \geq R_{th} \\ -\infty, & \text{otherwise} \end{cases} \tag{19}$$

The optimal assignment $\mathbf{X}^*$ is then efficiently obtained using the **Hungarian algorithm**. The complete execution flow of the algorithm is presented in Algorithm 1.

 doi:10.20944/preprints202603.2180.v1

Algorithm 1 Inner-Layer Task Assignment with QoS Guarantee

Input: The flight velocity of UAV $\mathbf{v} = \{v_m\}$; QoS throughput threshold R_{th}; Set of sensor nodes $\mathcal{K}_m$; Side length of each regular hexagonal cell R; UAV trajectory $\mathbf{q}(t)$.
Output: Optimal assignment matrix $\mathbf{X}^* = \{\mathbf{X}_m^*\}$ and total throughput $\Phi^* = \{\Phi_m^*\}$.

Initialize $N_m = |\mathcal{K}_m|$
for $m = 1$ to M do **do**
  Initialize cost matrix $\mathbf{C}_m$ of size $|\mathcal{N}_m| \times |\mathcal{K}_m|$
  for each slot index $i \in \mathcal{N}_m$ **do**
    Calculate current time: $t_i \leftarrow \frac{N_m+i}{2N_m} \times \frac{D}{v_m}$
    Obtain UAV position $\mathbf{q}(t_i)$ from trajectory
    for each node $k \in \mathcal{K}_m$ **do**
      Calculate channel gain $h_{m,k}(t)$ based on position $\mathbf{q}(t_i)$
      Calculate predicted throughput $C_{i,k}^m$
      if $C_{i,k}^m < R_{th}$ **then**
        $\tilde{C}_{i,k}^m \leftarrow -\infty$
      else
        $\tilde{C}_{i,k}^m \leftarrow C_{i,k}^m$
      end if
    end for
  end for
  Apply **Hungarian Algorithm** on $\tilde{\mathbf{C}}_m$ to find maximum weight matching
  Obtain the optimal binary assignment matrix $\mathbf{X}_m^*$ and Φ_m^*
  if $\Phi_m^* > -\infty$ **then**
    update $\mathbf{X}^*$ and Φ^*
  else
    return Infeasible ▷ Current velocity cannot satisfy QoS
  end if
end for
return $\mathbf{X}^*$ and Φ^*

5.2. Outer Layer: Velocity Optimization

Based on the theoretical foundation established in Theorem 2, the individual throughput strictly monotonically decreases with the UAV cruising velocity v_m. Consequently, the optimization objective seamlessly translates to finding the maximum feasible velocity v_m^* that tightly satisfies the worst-case QoS constraint, i.e., $\Phi_{\min}(v_m) \geq R_{th}$. The monotonic nature of the throughput guarantees that the feasible velocity region $[V_{\min}, v_m^*]$ is contiguous, allowing us to pinpoint the global optimum boundary precisely and efficiently.

Leveraging this physical insight, we propose a low-complexity bisection search for the outer-layer optimization. The core logic relies on the inner-layer Hungarian algorithm to serve as a feasibility checker: for a given test velocity, the inner layer verifies whether there exists a time-slot allocation strategy where the throughput of all nodes simultaneously satisfies the minimum threshold R_{th}.

As detailed in Algorithm 2, for each cell m, the algorithm first checks whether the maximum mechanical velocity $V_{\max}$ inherently yields a feasible allocation. If not, it initializes the search boundaries as $[V_{\min}, V_{\max}]$ and iteratively halves the search space. In each iteration, the mid-point velocity *mid* is passed to the inner layer. If a feasible allocation exists under *mid*, the outer algorithm attempts a higher speed to maximize the overall task efficiency; otherwise, it reduces the speed to guarantee data collection. This process rapidly converges to the boundary critical velocity v_m^*.

 doi:10.20944/preprints202603.2180.v1

Algorithm 2 Outer-Layer Optimization: Bisection Velocity Search

Input: Physical velocity limits $[V_{\min}, V_{\max}]$; Convergence tolerance ϵ_{bin}.
Output: Optimal velocity set $\mathbf{v}^* = \{v_m^*\}_{m=1}^{M}$.

for $m = 1 \to M$ **do**
  Run **Algorithm 1** with test velocity $V_{\max}$
  if Feasible allocation exists **then**
    $v_m^* \leftarrow V_{\max}$
  else
    $low \leftarrow V_{\min}$
    $high \leftarrow V_{\max}$
    while $(high - low) > \epsilon_{bin}$ **do**
      $mid \leftarrow (low + high)/2$
      Run **Algorithm 1** with test velocity mid
      if Feasible allocation exists ($\Phi_{\min} \geq R_{th}$) **then**
        $low \leftarrow mid$
      else
        $high \leftarrow mid$
      end if
    end while
    $v_m^* \leftarrow low$
  end if
end for
return $\mathbf{v}^*$

6. Simulation and Discussion

6.1. Simulation Setup

To evaluate the performance of the proposed STD-TDMA, extensive numerical simulations are conducted using MATLAB 2021b. The simulation process is developed and implemented based on an event-driven algorithm to accurately capture the dynamic interactions within the network. Unless otherwise specified, the main simulation parameters are summarized in Table 1.

Table 1. Simulation Parameters

Parameter	Value	Parameter	Value
Hexagonal cell side length R	10 m	System bandwidth B	1 MHz
UAV transmit power P_e	30 dBm	Reference channel gain β_0	-30 dB
QoS constraint R_{th}	300 kbits	Path loss exponent δ	2.8
UAV velocity range $[v_{\min}, v_{\max}]$	$[5, 15]$ m/s	Noise power σ^2	-110 dBm
Energy conversion efficiency ζ	0.7	A2G environmental params (a, b)	$(9.61, 0.16)$
Node max power P_{max}	5 μW	NLOS attenuation factor η	0.1

To comprehensively evaluate the performance of our proposed algorithm, we introduce three representative baseline schemes for comparison. The detailed operations of these baselines are defined as follows.

- **Baseline 1: Fixed TDMA Scheduling (F-TDMA):** In this multi-access scheduling scheme, the TDMA time slots are allocated to the sensor nodes in a predetermined, fixed sequence. The resource allocation order and the corresponding communication durations are statically assigned prior to the flight, regardless of the dynamic spatial-temporal channel variations during the UAV's movement.
- **Baseline 2: Non-Orthogonal Multiple Access Scheme (NOMA) [31]:** In the WIT phase, all nodes transmit simultaneously via NOMA. The UAV employs Successive Interference Cancellation (SIC) to decode signals in descending order of received power. To simulate realistic hardware constraints, an imperfect SIC model is adopted with a residual interference factor 1%.

 doi:10.20944/preprints202603.2180.v1

- **Baseline 3: Fly-Hover-Communicate Scheme (FHCS) [20]:** In the HAG scheme, the UAV flies directly to the geometric center of the target cell at its maximum velocity $v_{\max}$. Upon arrival, the UAV hovers stably at this central location to broadcast radio frequency energy and collect data from all nodes sequentially. To ensure comparative fairness, the time duration spent in each cell is strictly aligned with the time budget of our strategy.

6.2. Simulation Results

We first introduce our simulation network topology as illustrated in Figure 3. The UAV departs from the initial position (indicated by the red dot) and follows the blue trajectory to reach the destination (indicated by the green dot). Within each cell, sensor nodes are randomly distributed.

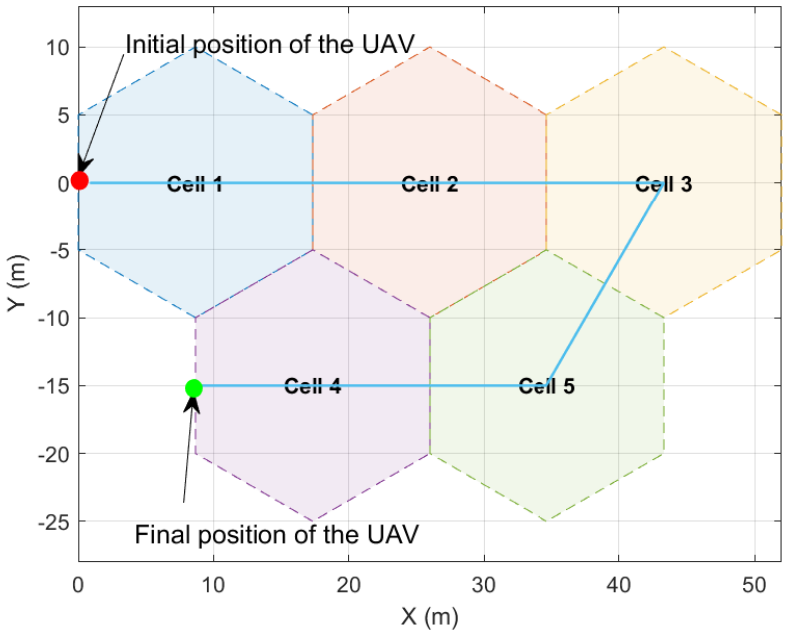

Figure 3. Simulation Network Topology.

Figure 4 illustrates the impact of UAV flight velocity on the average cell throughput for different scheduling schemes under varying flight altitudes ($H = 5$ m, 10 m, and 15 m), with a fixed network size of $N = 10$. From the presented results, three main observations can be drawn: (1) First, the average throughput decreases as the UAV flight velocity (V) increases. This is because a higher velocity reduces the total time the UAV stays in the cell, thus limiting the duration for both WET and WIT. This observation is consistent with the theoretical derivation in Theorem 2. (2) The proposed STD-TDMA scheme consistently outperforms all baseline schemes across the entire velocity regime. By exploiting the continuous flight trajectory and dynamically mapping nodes to their optimal spatio-temporal channel conditions, our proposed scheme maximizes the multi-access efficiency and achieves the optimal throughput even under stringent time budgets. (3) By comparing subfigures 4 (**a**), (**b**), and (**c**), it is evident that the overall throughput for all schemes noticeably declines as the UAV flight altitude (H) increases. This is highly intuitive, as a higher altitude inevitably incurs more severe path loss.

 doi:10.20944/preprints202603.2180.v1

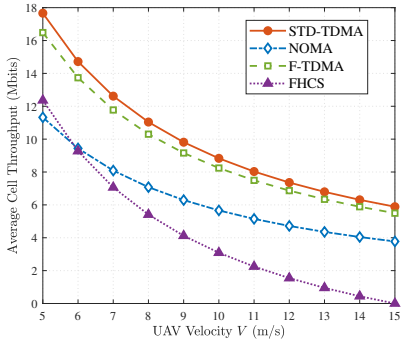

(**a**)

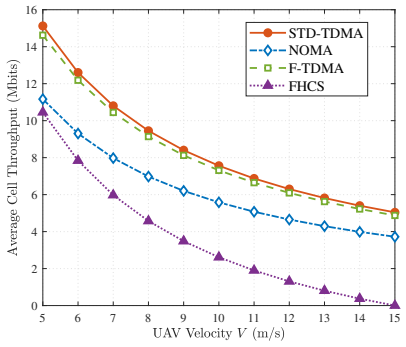

(**b**)

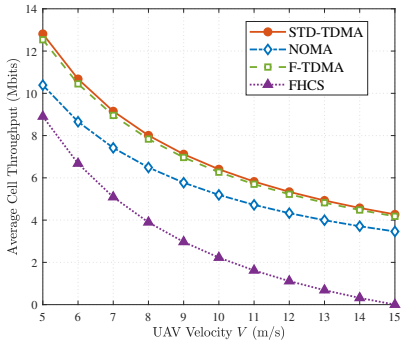

(**c**)

Figure 4. Average cell throughput versus UAV flight velocity under various flight altitudes. (**a**) Performance comparison at a UAV flight altitude of $H = 5$ m. (**b**) Performance comparison at a UAV flight altitude of $H = 10$ m. (**c**) Performance comparison at a UAV flight altitude of $H = 15$ m.

Figure 5 evaluates the average system utility versus the UAV flight velocity under varying flight altitudes ($H = 5$ m, 10 m, and 15 m), maintaining the same parameters as in Figure 4. Based on the simulation results, we can draw the following observations. (1) The proposed STD-TDMA scheme consistently achieves superior average utility across all evaluated velocities and altitudes compared to the baseline methods. (2) The average utility curves for the continuous "fly-and-communicate" paradigms—namely STD-TDMA, NOMA, and F-TDMA—remain remarkably flat and almost entirely unaffected by variations in the UAV flight velocity. This perfectly corroborates the mathematical derivations presented in Theorem 1. (3) Finally, while the average utility remains theoretically stable across velocities, an excessively high UAV speed drastically limits the staying time and the nodes' harvested energy. As previously evidenced by the sharp decline in absolute system throughput in Figure 4, disadvantaged nodes eventually fail to meet the minimum QoS constraint.

 doi:10.20944/preprints202603.2180.v1

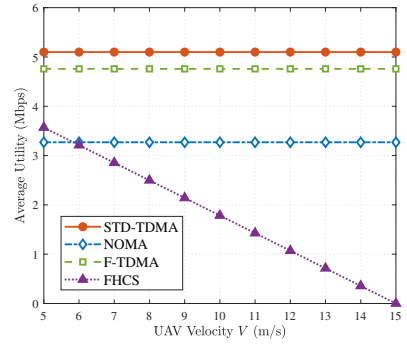

(**a**)

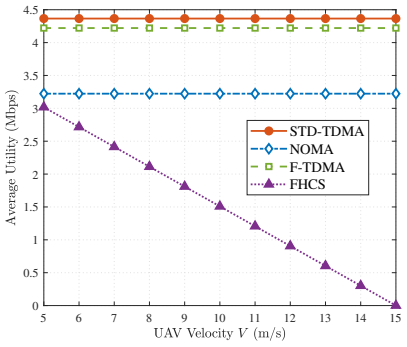

(**b**)

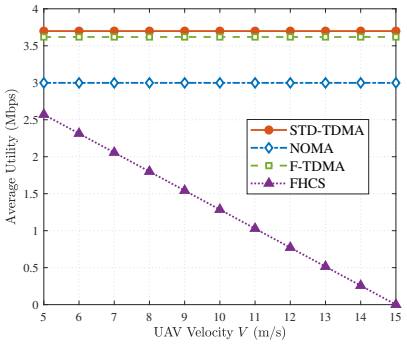

(**c**)

Figure 5. Average utility versus UAV flight velocity under various flight altitudes. (**a**) Performance comparison at a UAV flight altitude of $H = 5$ m. (**b**) Performance comparison at a UAV flight altitude of $H = 10$ m. (**c**) Performance comparison at a UAV flight altitude of $H = 15$ m.

Next, we evaluate the system performance of the considered scheduling schemes under varying network sizes (i.e., different numbers of sensor nodes), with the UAV flight velocity fixed at $V = 10$ m/s. As depicted in Figure 6, we have the following observations. (1) The proposed STD-TDMA scheme consistently demonstrates absolute superiority and maintains the highest average utility across all evaluated network scales. (2) As the number of sensor nodes increases, the data collection efficiency of our proposed scheme exhibits a significantly more pronounced growth margin compared to the baseline methods. This substantial improvement highlights the excellent scalability of STD-TDMA. By dynamically matching nodes to their optimal spatio-temporal slots, our scheme effectively exploits the multi-user diversity inherent in denser networks, thereby maximizing the overall system efficiency as the network scales up.

To provide a more granular perspective on user fairness, Figure 7 presents the cumulative distribution function (CDF) of individual node throughput under various UAV flight altitudes, with

 doi:10.20944/preprints202603.2180.v1

all system parameters remaining identical to those in Figure 6. In these statistical plots, a coordinate (x, y) mathematically indicates that a proportion y of the total sensor nodes achieves a throughput less than or equal to the value x. Based on this definition, several critical observations can be drawn: (1) Our proposed STD-TDMA exhibits the steepest CDF curve among all methods. This indicates the smallest throughput variation among the nodes, proving that our strategy achieves the maximum system fairness. (2) The CDF curve of STD-TDMA consistently starts to the right of the threshold . This confirms that every single node successfully satisfies the minimum QoS constraint.

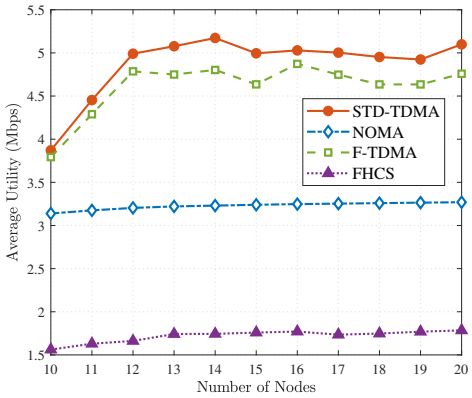

(**a**)

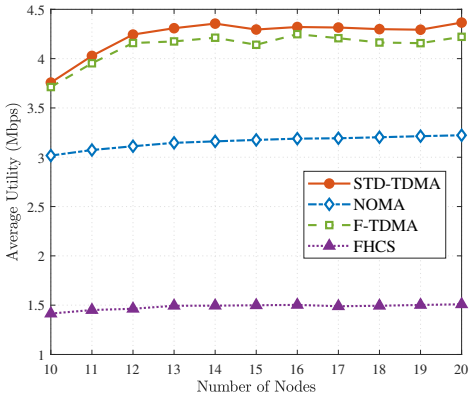

(**b**)

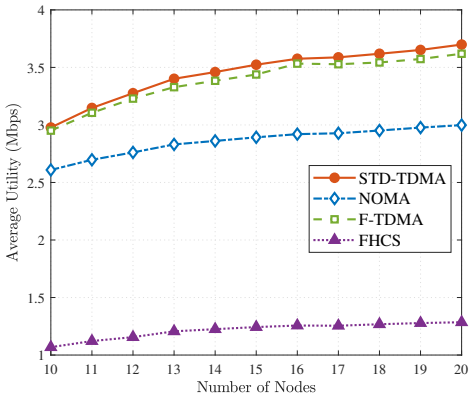

(**c**)

Figure 6. Average utility versus the number of sensor nodes under various flight altitudes. (**a**) Performance comparison at a UAV flight altitude of $H = 5$ m. (**b**) Performance comparison at a UAV flight altitude of $H = 10$ m. (**c**) Performance comparison at a UAV flight altitude of $H = 15$ m.

 doi:10.20944/preprints202603.2180.v1

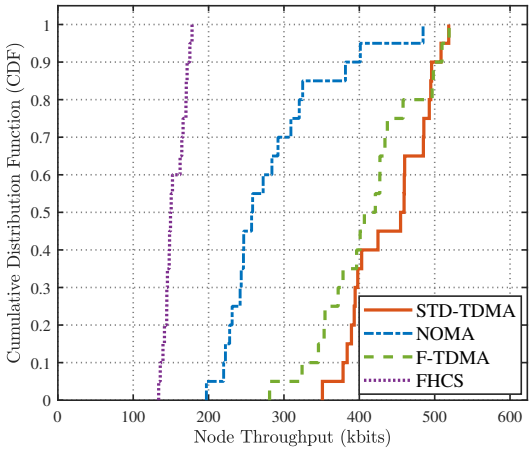

(**a**)

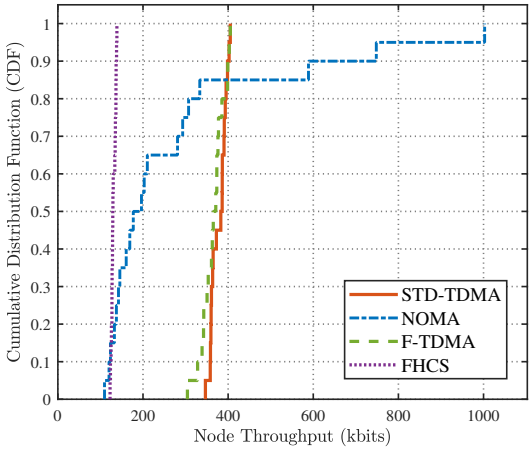

(**b**)

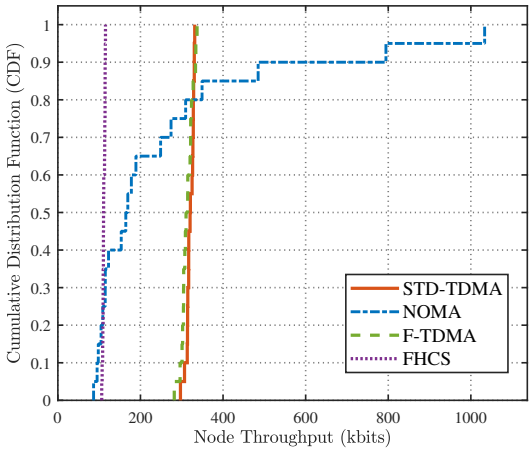

(**c**)

Figure 7. Cumulative distribution function of individual node throughput under various UAV flight altitudes. (**a**) Performance comparison at a UAV flight altitude of $H = 5$ m. (**b**) Performance comparison at a UAV flight altitude of $H = 10$ m. (**c**) Performance comparison at a UAV flight altitude of $H = 15$ m.

Finally, to provide microscopic insights into the effectiveness of the proposed STD-TDMA scheduling, we characterize the individual nodal throughputs and the spatio-temporal channel gain evolution

 doi:10.20944/preprints202603.2180.v1

over the entire UAV execution period within a randomly generated target cell. As explicitly shown in Figure 8, to strictly guarantee system-wide fairness, our proposed STD-TDMA intelligently allocates the peak channel gain slots (e.g., time slot 20) to the inherently disadvantaged nodes (e.g., Node 7). This dynamic mapping mechanism effectively compensates for their severe spatial path loss, ensuring that even the worst-case nodes successfully satisfy the minimum QoS constraint (R_{th}).

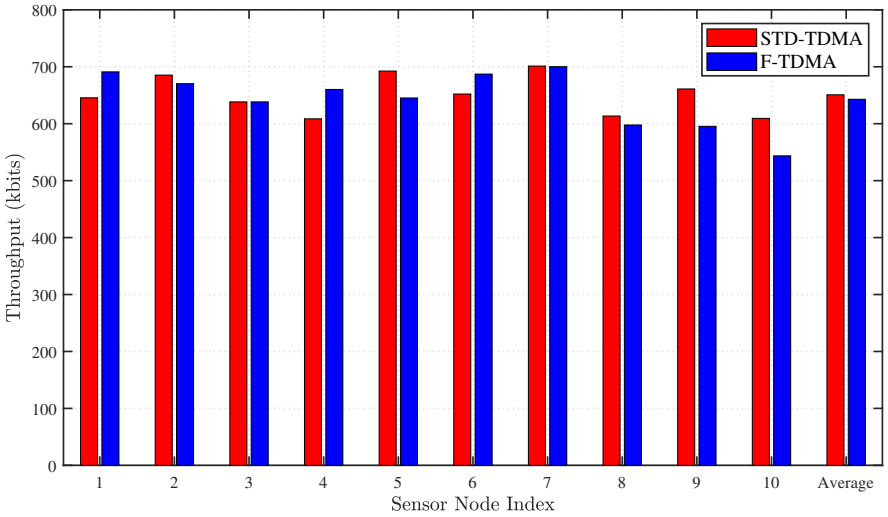

(**a**)

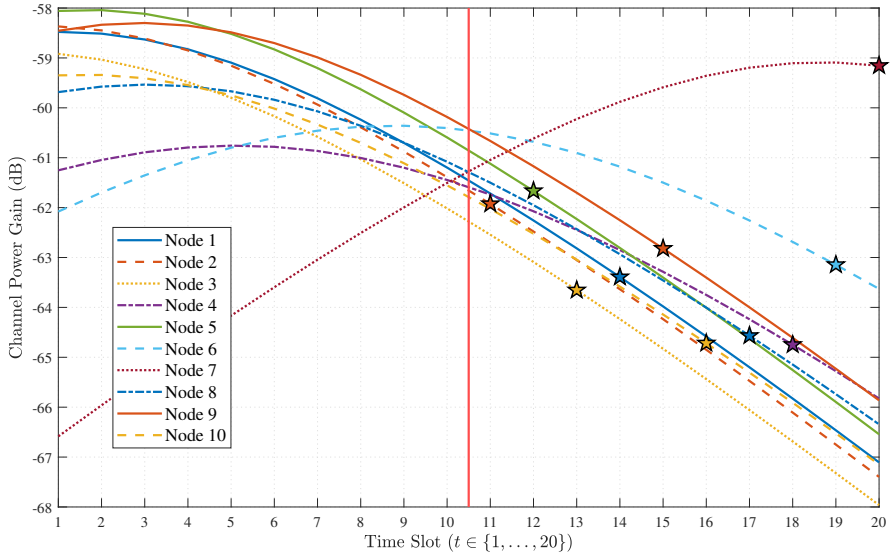

(**b**)

Figure 8. Detailed node-level performance and channel gain evolution within a target cell under the baseline scenario parameters ($N = 10$, $H = 10$ m, and $V = 10$ m/s). (**a**) Individual and average nodal throughput comparison. (**b**) Spatio-temporal channel power gain profiles for all 10 sensor nodes across the 20 continuous time slots.

7. Conclusions

In this paper, we proposed a novel Spatio-Temporal Dynamic Time Division Multiple Access scheduling scheme for UAV-assisted WPCNs to tackle the severe "doubly near-far" problem. Simulation results demonstrate that STD-TDMA significantly outperforms benchmark schemes in both average system utility and fairness. By intelligently allocating peak channel gain slots to disadvantaged nodes,

 doi:10.20944/preprints202603.2180.v1

our scheme effectively eliminates spatial data holes and strictly guarantees the QoS requirements for all nodes.

Currently, our framework assumes a predetermined UAV trajectory. In future work, we plan to integrate Deep Reinforcement Learning (DRL) algorithms for autonomous UAV trajectory planning. Jointly optimizing the DRL-based dynamic path planning with the STD-TDMA resource allocation will further enhance the network's adaptability and overall performance in complex, dynamic environments.

Author Contributions: Conceptualization, S.G. and K.Q.; methodology, S.G., K.Q. and Q.C.; software, Y.W., S.G.; validation, S.G., H.W., H.H., P.Q. and Q.C.; formal analysis, S.G., P.Q. and Q.C.; writing—original draft preparation, S.G., K.Q. and H.W.; writing—review and editing, S.G. and Q.C.; supervision, S.G. and H.H.; project administration, S.G. and Q.C.; funding acquisition, S.G., K.Q. and Q.C.; All authors have read and agreed to the published version of the manuscript.

Funding: This work was supported in part by the Zhejiang Provincial Education Department Project under Grant jg20230057, the Zhejiang Provincial Natural Science Foundation of China under Grant LQ23F020004, the Wenzhou Municipal Science and Technology Bureau Project under Grant G2023002, the Henan Provincial Science and Technology Research Project under Grants 252102220039, 252102211068, and 252102210110, the Key Research Project Plan for Higher Education Institutions of Henan Province under Grant 24A520027, the Natural Science Foundation of China under Grant 62502242.

Data Availability Statement: The original contributions presented in this study are included in the article. Further inquiries can be directed to the corresponding authors.

Conflicts of Interest: The authors declare no conflicts of interest.

Abbreviations

The following abbreviations are used in this manuscript:

UAV	Unmanned aerial vehicle
WPCN	Wireless powered communication network
SN	Sensor node
EH	Energy harvesting
RF	Radio frequency
QoS	Quality of service
WET	Wireless energy transfer
WIT	Wireless information transmission
OFDMA	Orthogonal frequency division multiple access
NOMA	Non-Orthogonal multiple access
TDMA	Time-division multiple access
LoS	Line-of-sight
NLoS	Non-line-of-sight
A2G	Air-to-ground

References

1. Wang, Y.; Zu, K.; Xiang, L.; Zhang, Q.; Feng, Z.; Hu, J.; Yang, K. ISAC Enabled Cooperative Detection for Cellular-Connected UAV Network. *IEEE Trans. Wireless Commun.* **2025**, *24*, 1541–1554.
2. Nemati, M.; Al Homssi, B.; Krishnan, S.; Park, J.; Loke, S.W.; Choi, J. Non-Terrestrial Networks with UAVs: A Projection on Flying Ad-Hoc Networks. *Drones* **2022**, *6*, 334.
3. Chen, Z.; Guo, Y.; Hao, J.; Du, Y. Energy Efficient UAV Trajectory Design for Hovering-Flying Data Collection. In Proceedings of the *2022 IEEE Globecom Workshops (GC Wkshps)*, 2022; pp. 886–890.
4. Tang, H.; Wu, Q.; Chen, W.; Wang, J.; Li, B. Mitigating the Doubly Near–Far Effect in UAV-Enabled WPCN. IEEE Trans. Veh. Technol. 2021, 70, 8349–8354.
5. Gu, X.; Zhang, G. A survey on UAV-assisted wireless communications: Recent advances and future trends. *Comput. Commun.* **2023**, *208*, 44-78.

 doi:10.20944/preprints202603.2180.v1

6. Zeng, Y.; Zhang, R.; Lim, T.J. Throughput Maximization for UAV-Enabled Mobile Relaying Systems. *IEEE Trans. Commun.* **2016**, *64*, 4983–4996.
7. Wu, Q.; Zeng, Y.; Zhang, R. Joint Trajectory and Communication Design for Multi-UAV Enabled Wireless Networks. *IEEE Trans. Wireless Commun.* **2018**, *17*, 2109–2121.
8. Wang, Y.; Gao, Z.; Zhang, J.; Cao, X.; Zheng, D.; Gao, Y.; Ng, D.W.K.; Di Renzo, M. Trajectory Design for UAV-Based Internet of Things Data Collection: A Deep Reinforcement Learning Approach. *IEEE Internet Things J.* **2022**, *9*, 3899–3912.
9. Abou Arkoub, M.; Hamdi, R.; Qaraqe, M. Trajectory Optimization for UAV-based Communication Systems Powered by Energy Harvesting. In Proceedings of the 2024 IEEE 100th Vehicular Technology Conference (VTC2024-Fall), Washington, DC, USA, 7–10 October 2024; pp. 1–6.
10. Zhang, L.; Celik A.; Dang, S.; Shihada, B. Energy-Efficient Trajectory Optimization for UAV-Assisted IoT Networks. *IEEE Trans. Mobile Comput.* **2022**, *21*, 4323-4337.
11. Qi, H.; Wu, M.; Zhang, Z.; Zhao, M. Trajectory Design for Multi-UAV-Enabled Wireless Powered Communication Networks: A Multi-Agent DRL Approach. In Proceedings of the 2024 IEEE Wireless Communications and Networking Conference (WCNC), Dubai, United Arab Emirates, 21–24 April 2024; pp. 1–6.
12. Xie, L.; Cao, X.; Xu, J.; Zhang, R. UAV-Enabled Wireless Power Transfer: A Tutorial Overview. *IEEE Trans. Green Commun. Netw.* **2021**, *5*, 2042–2064.
13. Xie, L.; Xu, J.; Zhang, R. Throughput Maximization for UAV-Enabled Wireless Powered Communication Networks. *IEEE Internet Things J.* **2019**, *6*, 1690–1703.
14. Cho, S.; Lee, K.; Kang, B.; Koo, K.; Joe, I. Weighted Harvest-Then-Transmit: UAV-Enabled Wireless Powered Communication Networks. *IEEE Access* **2018**, *6*, 72212-72224.
15. Li, M.; Cheng, N.; Gao, J.; Wang, Y.; Zhao, L.; Shen, X. Energy-Efficient UAV-Assisted Mobile Edge Computing: Resource Allocation and Trajectory Optimization. *IEEE Trans. Veh. Tech.* **2020**, *69*, 3424-3438.
16. Luo, W.; Shen, Y.; Yang, B.; Wang, S.; Guan, X. Joint 3-D Trajectory and Resource Optimization in Multi-UAV-Enabled IoT Networks With Wireless Power Transfer. *IEEE Internet Things J.* **2021**, *8*, 7833-7848.
17. Perera, T.D.P.; Panic, S.; Jayakody, D.N.K.; Muthuchidambaranathan, P. UAV-assisted Data Collection in Wireless Powered Sensor Networks over Multiple Fading Channels. In Proceedings of the IEEE International Conference on Computer Communications, Toronto, ON, Canada, 6–9 July 2020; pp. 1–6.
18. Sun, P.F.; Song, Y.; Gao, K.; Wang, Y.; Zhou, C.; Jeon, S.W.; Zhang, J. 3D UAV Trajectory Planning for IoT Data Collection Over 3D Terrain Features. In Proceedings of the 2025 IEEE 101st Vehicular Technology Conference (VTC2025-Spring), Oslo, Norway, 2025, pp. 1-6.
19. Liu, X.; Liu, H.; Zheng, K.; Liu, J.; Taleb, T.; Shiratori, N. AoI-Minimal Clustering, Transmission and Trajectory Co-Design for UAV-Assisted WPCNs. *IEEE Trans. Veh. Tech.* **2025**, *74*, 1035-1051.
20. Wu, P.; Yuan, X.; Hu, Y.; Schmeink, A. Joint Power Allocation and Trajectory Design for UAV-Enabled Covert Communication. *IEEE Trans. Wireless Commun.* **2024**, *23*, 683–698.
21. Lyu, J.; Zeng, Y.; Zhang, R. Common Throughput Maximization in UAV-Enabled OFDMA Systems With Delay Consideration. *IEEE Trans. Commun.* **2018**, *66*, 6614–6627.
22. An, Z.; Liu, Y.; Sun, G.; Pan, H.; Wang, A. UAV-enabled Wireless Powered Communication Networks: A Joint Scheduling and Trajectory Optimization Approach. In Proceedings of the 2022 IEEE Symposium on Computers and Communications (ISCC), Rhodes, Greece, 30 June–3 July 2022; pp. 1–6.
23. Park, J.; Lee, H.; Eom, S.; Lee, I. UAV-Aided Wireless Powered Communication Networks: Trajectory Optimization and Resource Allocation for Minimum Throughput Maximization. *IEEE Access* **2019**, *7*, 134978–134991.
24. Tang, Q.; Yang, Y.; Liu, L.; Yang, K. Minimal Throughput Maximization of UAV-enabled Wireless Powered Communication Network in Cuboid Building Perimeter Scenario. *IEEE Trans. Netw. Service Manag.* **2023**, *20*, 4558–4571.
25. He, Y.; Xiang, K.; Cao, X.; Guizani, M. Task Scheduling and Trajectory Optimization Based on Fairness and Communication Security for Multi-UAV-MEC System. *IEEE Internet Things J.* **2024**, *11*, 30510–30524.
26. Zhou, X.; Huang, L.; Ye, T.; Sun, W. Computation Bits Maximization in UAV-Assisted MEC Networks With Fairness Constraint. *IEEE Internet Things J.* **2022**, *9*, 20997-21009.
27. Al-Hourani, A.; Kandeepan, S.; Jamalipour, A. Modeling air-to-ground path loss for low altitude platforms in urban environments. In Proceedings of the 2014 IEEE Global Communications Conference, Cape Town, South Africa, 8–12 December 2014; pp. 2898–2904.
28. Jiang, Y.; Zhai, L.; Wu, T.; Li, B.; Zou Y.; Yan, P. Energy-Efficiency Optimization for RIS-Assisted UAV-Enabled IoT Networks, *IEEE Internet of Things J.*, 2025, 12, 42599-42612.

 doi:10.20944/preprints202603.2180.v1

29. Shen, X.; Gu, L.; Yang, J.; Shen, S. Energy Efficiency Optimization for UAV-RIS-Assisted Wireless Powered Communication Networks. Drones 2025, 9, 344.
30. Ju, H.; Zhang, R. Throughput Maximization in Wireless Powered Communication Networks. *IEEE Trans. Wirel. Commun.* 2014, 13, 407–421.
31. Shao, W., Lin, F., Xu, R., Meng, F., Wang, H. UAV-Assisted NOMA Network Power Allocation Under Offshore Multi-energy Complementary Power Generation System.Lecture Notes in Electrical Engineering, 2024:125-136.